MARTIAN MANTLE MELTING: A GEOCHEMICAL AND GEODYNAMIC PERSPECTIVE. M. S. Duncan[1] and M. B. Weller[2], [1]Virginia Tech, Dept. of Geosciences, 926 W. Campus Dr., Blacksburg, VA, (msduncan19@vt.edu), [2]Lunar and Planetary Institute/USRA, 3600 Bay Area Blvd, Houston, TX 77058 (mweller@lpi.usra.edu).

Introduction: Mantle melting is a fundamental process of planetary formation and evolution. Mars presents a unique case to track mantle melting throughout a planets' history as the ancient igneous surface is preserved [1-3]] and volcanic activity has continued throughout its history [1-3], potentially into the modern day [4,5].

Mantle melting calculations typically follow one of two paths: the geochemical or the geophysical. The geochemical process is usually derived from experimental results [e.g., 6] and allows calculation of F as a function of pressure (P) and temperature (T), as well as the melt composition (X), which can then be compared to the erupted lavas. This method takes into account the nonlinearity of F with temperature. It is limited by the extent of the experimental data, in P-T-X space. The geophysical approach typically assumes a linear distribution of F between the solidus and liquidus temperature [e.g., 7]. It does not result in a melt composition, but often will result in a melt volume that can be compared with erupted lavas. Here we begin to reconcile the differences between the two approaches in order to understand the observations of Mars.

Methods: All melt fractions (F) reported here are global averages. This means that F can equal 0, but melting is still occurring at hotspots.

Our techniques use much of the same input data including: the concentrations of the Heat Producing Elements (HPE: K, Th, U) [8,9], thermal conductivity (k), density, and crustal thickness.

Geochemical. We calculated areotherms (martian temperature profiles) through time as described previously [10]. This method uses surface heat flow (q_0) as an input, which is an output of our geodynamic models. Melt fraction was calculated from our geochemical 1D thermal model using:

$$F = \left[\left(\frac{dT}{dP_{solidus}} - \frac{dT}{dP_{adiabat}}\right)/\left(\frac{\Delta H_F}{C_P} + \frac{dT}{dF}\right)\right](P_0 - P_F)$$

where P_0 is the pressure in GPa where the solidus intersects the adiabat, which indicates the initiation of melt production, P_F is the pressure at the cessation of melt production and is marked by the intersection of the adiabat and the areotherm, $dT/dP_{solidus}$ is the slope of the solidus ~106.15 K/GPa over the pressure range here [11], $dT/dP_{adiabat}$ is the slope of the adiabat 0.18 K/km [12], ΔH_F is the enthalpy of fusion 6.4×10^5 J/kg [12], C_P is the heat capacity 1200 J/K kg [12], and dT/dF is the change in T as a function of F and was calculated from previous experimental data [13-15], and ranged from 4.38 to 3.9 K/F depending on pressure. Adiabats through time were taken from [16], where the mantle potential temperatures were determined from martian meteorites and surface basalts.

Geodynamic. We used CitcomS [17] to calculate volumetrically averaged mantle areotherms for boundary constraints in the areotherm modeling. CitcomS is a robust and well benchmarked code that utilizes fully spherical 3D and dynamic domains of the whole mantle, as opposed to the 1D models required by the geochemical calculations. These profiles employed a constant boundary temperature at the surface (T = 220 K) and at the CMB (T = 1828 K); with an adiabatic gradient of 0.18 K/km [12]) and a basally defined Rayleigh number of 3×10^6. The viscosity contrast between the mantle and core is fixed at -3×10^5. Boundary conditions are free slip. We considered variable internal heating rates (Q), a proxy for either time or chemical depletion, and a core fraction (f) of 0.54 of the total planetary radius, consistent with the results from the InSight mission [18]. From these profiles, we determined average q_0 and melt fraction as a function of time. These q_0 were input into the geochemical framework allowing for the calculation of melt fraction using the geochemical approach.

Geodynamic melt fraction was calculated following the approach of [19]:

$$F = T' + (T'^2 - 0.25)(0.4256 + 2.988T') + 0.5$$

and

$$T' = {(T - T_s)}/{(T_l - T_s)}$$

where T_s is the solidus temperature, T_l is the liquidus temperature and T is the model temperature, all at the same pressure.

Results: Initial results show the differences between the two approaches. The averaged areotherms from CitcomS are generally colder than those calculated using the geochemical approach with the q_0 from the CitcomS output (Figure 1). The main differences likely arise from the 1D nature of the geochemical approach and 3D nature of the CitcomS results where melting occurs at the tops of plumes (Figure 2). These early results also show that the 3D geodynamic simulations predict on average higher melt fractions of a parcel than the 1D geochemical counterparts (Figure 3).

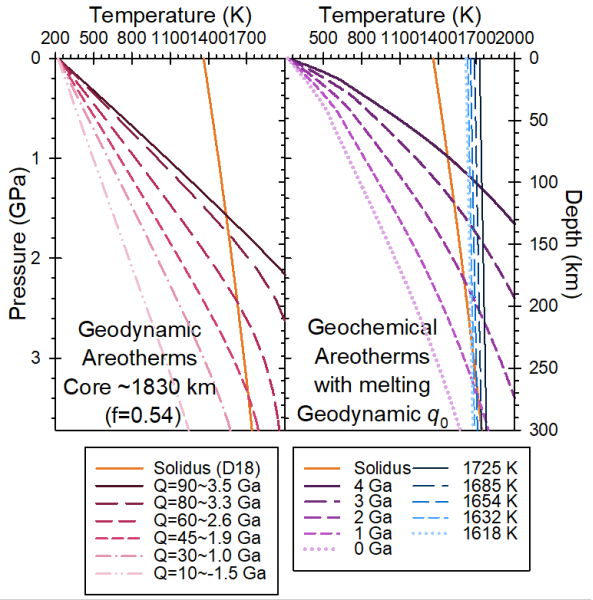

Figure 1. Calculated areotherms from CitcomS (left) and following the geochemical procedure using the surface heat flux output from CitcomS (right). Blue lines are adiabats [16] for each geochemical timestep.

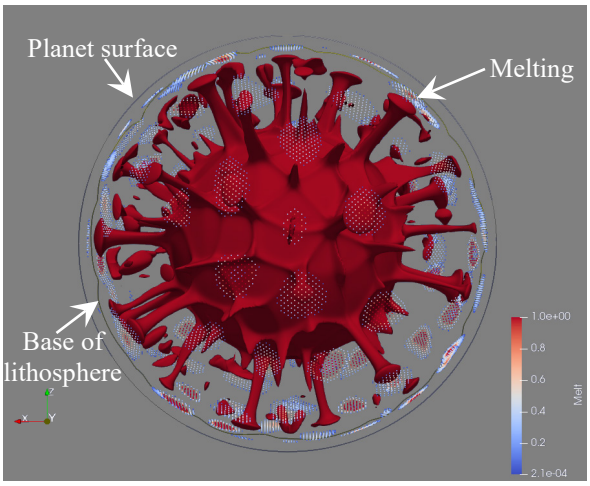

Figure 2. CitcomS result for Q = 30 ~ 1.0 Ga, F = 0.26. Melt occurs where the plumes intersect the solidus. Melt is denoted by the stippled zones and is color coded from 3.2×10^{-7} to 0.43. The red surface is temperature as an isocontour plot in 3D of 0.935 nondimensional T; 1496 K non adiabatic. The outer circle is the surface of the planet. The inner circle is the bottom of the lithosphere – at a radius of 0.935, or ~220 km. Note, melting occurs in discrete plumes.

Conclusions/Implications: Currently, geodynamic models predict much larger amounts of melting than the geochemical approach, even though the geochemical areotherms are generally warmer than those derived from the CitcomS results. Both techniques average from the onset (crossing the solidus) to cessation of melting. The key difference between them seems to be that the 3D simulations allow for 3D plume structures to develop, and allow for the entrainment of hot mantle along the core mantle boundary into the plume – ascending and melting towards the lithosphere boundary. On average, the material that melts in the 3D simulations does so at a higher fluxing rate, and at higher temperatures, corresponding then to higher melt fractions. While the simulations are not exactly the same (e.g., 3D simulations do not currently allow for the coupled thermal evolution with melt), this might suggest that 1D simulations underpredict melt generation. We are currently evaluating the robustness of this result. However, given the nature of the 1D code, an F=0 today does not preclude melting in hotspots, just that the overall mantle is not melting, consistent with current observations.

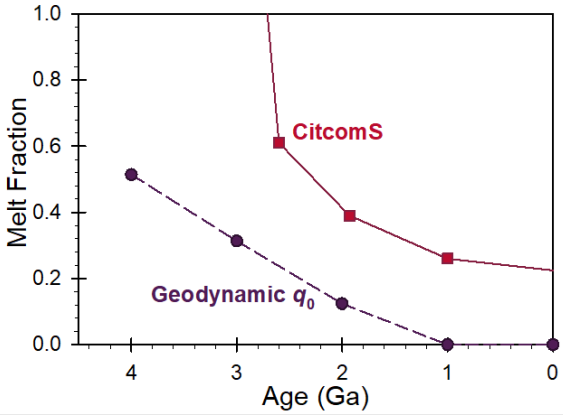

Figure 3. Calculated average melt fraction as a function of time. The purple dashed line and circles correspond to the geochemical model in Figure 1. The solid red line and squares correspond to the CitcomS results. Both models show decreasing F with time.

References: [1] Grott et al. (2013) *Space Sci. Rev.* [2] Hartmann. (2005) *Icarus*. [3] Werner. (2009) *Icarus*. [4] Horvath et al. (2021) *Icarus*. [5] Moitra et al. (2021) *EPSL*. [6] Duncan et al. (2017) *EPSL*. [7] Morschhauser et al. (2011) *Icarus*. [8] Dreibus and Wänke. (1985) *Meteor*. [9] Taylor and McLennan. (2009) *Planetary Crusts*. [10] Duncan et al. (2022) 53rd LPSC. [11] Duncan et al. (2018) *GRL*. [12] Kiefer. (2003) *MaPS*. [13] Matsukage et al. (2013) *J. Min. Pet. Sci.* [14] Collinet et al. (2015) *EPSL*. [15] Collinet et al. (2021) *JGR*. [16] Filiberto. (2017) *CG*. [17] Zhong et al. (2000) *JGR*. [18] Stähler et al. (2021) *Sci.* [19] McKenzie and Bickle (1988) *J. Petrol.*